

# Atypical Protein Kinase C $\alpha$ Is Required for Bronchioalveolar Stem Cell Expansion and Lung Tumorigenesis

Roderick P. Regala,<sup>1</sup> Rebecca K. Davis,<sup>1</sup> Alyssa Kunz,<sup>1</sup> Andras Khor,<sup>2</sup> Michael Leitges,<sup>3</sup> and Alan P. Fields<sup>1</sup>

Departments of <sup>1</sup>Cancer Biology and <sup>2</sup>Pathology, Mayo Clinic Comprehensive Cancer Center, Jacksonville, Florida and <sup>3</sup>Biotechnology Centre of Oslo, University of Oslo, Oslo, Norway

## Abstract

**Protein kinase C $\alpha$  (PKC $\alpha$ ) is an oncogene required for maintenance of the transformed phenotype of non-small cell lung cancer cells. However, the role of PKC $\alpha$  in lung tumor development has not been investigated. To address this question, we established a mouse model in which oncogenic *Kras*<sup>G12D</sup> is activated by Cre-mediated recombination in the lung with or without simultaneous genetic loss of the mouse PKC $\alpha$  gene, *Prkci*. Genetic loss of *Prkci* dramatically inhibits *Kras*-initiated hyperplasia and subsequent lung tumor formation *in vivo*. This effect correlates with a defect in the ability of *Prkci*-deficient bronchioalveolar stem cells to undergo *Kras*-mediated expansion and morphologic transformation *in vitro* and *in vivo*. Furthermore, the small molecule PKC $\alpha$  inhibitor aurothiomalate inhibits *Kras*-mediated bronchioalveolar stem cell expansion and lung tumor growth *in vivo*. Thus, *Prkci* is required for oncogene-induced expansion and transformation of tumor-initiating lung stem cells. Furthermore, aurothiomalate is an effective antitumor agent that targets the tumor-initiating stem cell niche *in vivo*. These data have important implications for PKC $\alpha$  as a therapeutic target and for the clinical use of aurothiomalate for lung cancer treatment. [Cancer Res 2009;69(19):7603–11]**

## Introduction

Lung cancer is the leading cause of cancer death in the United States (1). Non-small cell lung cancer (NSCLC) is the most prevalent type of lung cancer accounting for ~80% of cases (2). Despite recent treatment advances, the 5-year survival rate of patients with NSCLC remains only 15%. Thus, there is a dire need to better understand the key molecular events driving lung tumorigenesis that could lead to more effective means of prevention, diagnosis, prognosis, and treatment.

Activating mutations in *Kras* are among the most common molecular changes found in NSCLC tumors (3, 4) and several transgenic mouse models have shown the critical role of oncogenic *Kras* in lung tumor initiation and maintenance. Transgenic mice carrying a conditional oncogenic *Kras*<sup>G12D</sup> allele activated by Cre-recombinase (*LSL-Kras* mice) develop epithelial hyper-

plasias, lung adenomas, and adenocarcinomas (5, 6). A second murine lung cancer model (the *Kras*<sup>LA</sup> mouse) is based on sporadic *Kras* mutation using a “hit-and-run” gene targeting strategy (7). *Kras*<sup>LA</sup> mice carry a latent activation oncogenic *Kras*<sup>G12D</sup> allele activated by spontaneous somatic recombination. *Kras*<sup>LA</sup> mice invariably develop numerous lung tumors pathologically similar to human disease (7).

Bronchioalveolar stem cells (BASC) are the probable cells of origin of *Kras*-induced lung tumors in these mouse models (8). BASCs function in lung homeostasis and possess characteristics of regional lung stem cells (8). BASCs reside in bronchioalveolar duct junctions (BADJ), a niche at the boundary between the terminal bronchioles (TB) and the alveolar space. BASCs express the hematopoietic stem cell marker Sca-1, Clara cell-specific protein (CCSP), and surfactant protein C (SPC), but not the hematopoietic and endothelial cell markers CD45 and Pecam (8). BASCs exhibit stem-like self-renewal and the ability to differentiate into Clara cells and alveolar type II (AT2) cells *in vitro* (8). Moreover, BASCs expand in response to *Kras* transformation *in vitro*, and within the BADJ *in vivo*, eventually giving rise to adenomas and carcinomas in the *LSL-Kras* mouse model (8).

We recently showed that protein kinase C $\alpha$  (PKC $\alpha$ ) is an oncogene in NSCLC (9, 10). PKC $\alpha$  expression is elevated in NSCLC tumors and cell lines, and PKC $\alpha$  is required for the transformed phenotype of NSCLC cells harboring oncogenic *Kras* mutation (9). PKC $\alpha$  activates a novel oncogenic PKC $\alpha$ -Par6-Rac1 signaling axis that is necessary for the maintenance of the transformed phenotype of human NSCLC cells (11). We recently identified aurothiomalate as a potent and selective inhibitor of oncogenic PKC $\alpha$  signaling (12, 13). Aurothiomalate inhibits NSCLC cell transformation *in vitro* and tumorigenicity *in vivo* by disrupting the interaction between PKC $\alpha$  and Par6, thereby blocking the PKC $\alpha$ -Par6-Rac1 signaling axis (12, 13).

Although PKC $\alpha$  is important in the maintenance of the transformed phenotype of NSCLC cells harboring *Kras* mutation (11, 14), the role of PKC $\alpha$  in *Kras*-mediated lung tumor development has not been explored. Here, we assess the role of the mouse PKC $\alpha$  gene *Prkci*, in *Kras*-mediated lung tumorigenesis using a novel bitransgenic mouse model harboring conditional *LSL-Kras* and *Prkci* knockout (*Prkci*<sup>fl/fl</sup>) alleles. *LSL-Kras/Prkci*<sup>fl/fl</sup> mice exhibit a significant impairment in lung hyperplasia and lung tumor formation, indicating that *Prkci* is necessary for early events in *Kras*-mediated lung tumorigenesis. The effect of *Prkci* deficiency on tumorigenesis correlates with a defect in *Kras*-mediated BASC expansion in the absence of *Prkci*. Furthermore, the PKC $\alpha$  inhibitor aurothiomalate inhibits *Kras*-mediated BASC expansion and transformation *in vitro* and *in vivo*. Our results show that *Prkci* plays a requisite role in BASC transformation and identify aurothiomalate as a promising therapeutic agent that can target the lung cancer stem cell niche *in vivo*.

**Note:** Supplementary data for this article are available at Cancer Research Online (<http://cancerres.aacrjournals.org/>).

A.P. Fields and M. Leitges are both communicating authors.

**Requests for reprints:** Alan P. Fields, Department of Cancer Biology, Mayo Clinic Comprehensive Cancer Center, Griffin Cancer Research Building, Room 212, 4500 San Pablo Road, Jacksonville, FL 32224. Phone: 904-953-6109; Fax: 904-953-0277; E-mail: fields.alan@mayo.edu.

©2009 American Association for Cancer Research.  
doi:10.1158/0008-5472.CAN-09-2066

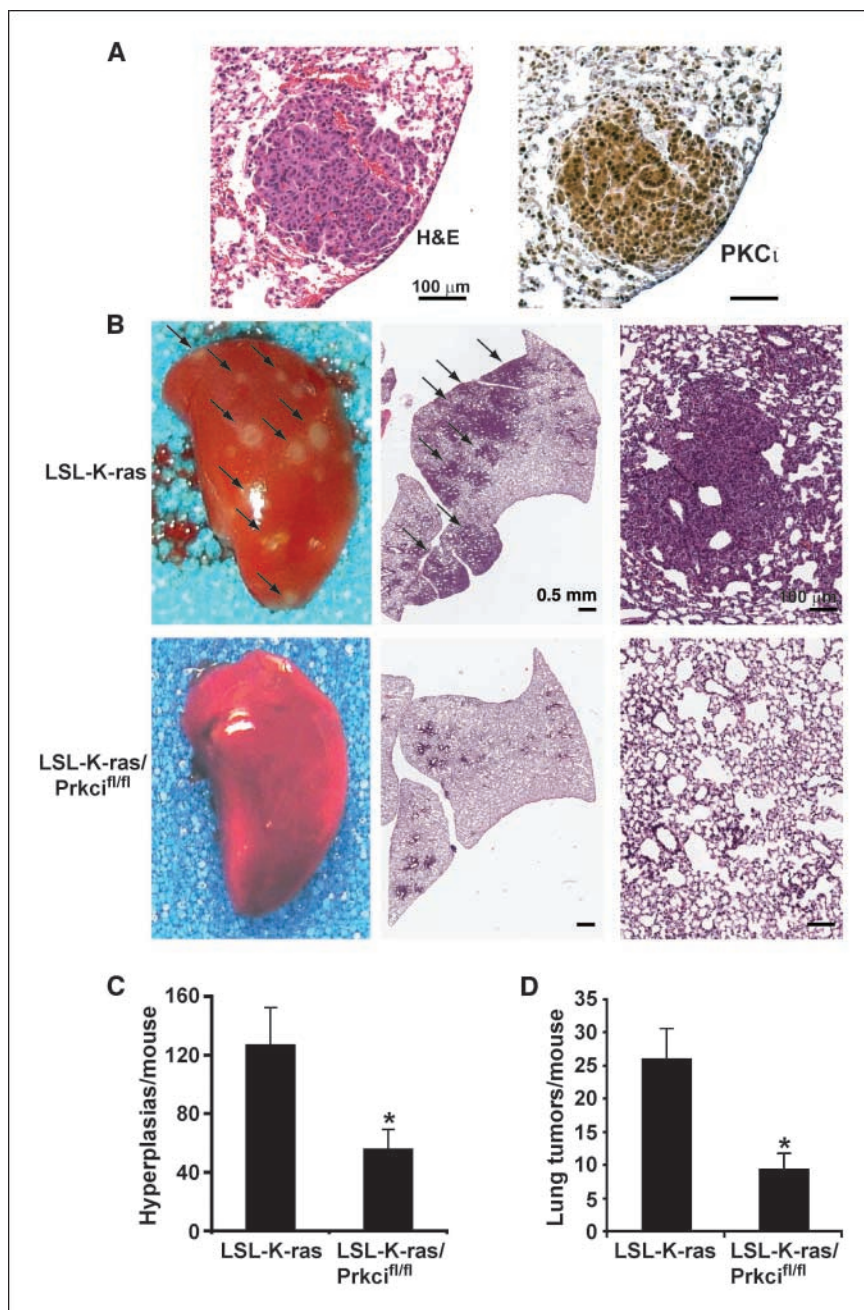


**Figure 1.** *Prkci* is necessary for *Kras*-mediated lung tumorigenesis. *LSL-Kras* and *LSL-Kras/Prkci<sup>fl/fl</sup>* mice were infected with AdCre, harvested, and processed as described in the Materials and Methods. **A**, staining of a *LSL-Kras* lung tumor for mouse PKC $\iota$  protein. **B**, histopathology of *LSL-Kras* and *LSL-Kras/Prkci<sup>fl/fl</sup>* mice. **Top left**, multiple lesions are evident on the surface of *LSL-Kras* mouse lungs (arrows). **Top middle**, *LSL-Kras* mice develop numerous focal adenomas (arrows). **Top right**, *LSL-Kras* adenomas often surround bronchioles. **Bottom left**, *LSL-Kras/Prkci<sup>fl/fl</sup>* mice exhibit a smooth lung surface devoid of visible lesions. **Bottom middle**, *LSL-Kras/Prkci<sup>fl/fl</sup>* lungs exhibit fewer and smaller lesions than *LSL-Kras* mice. **Bottom right**, *LSL-Kras/Prkci<sup>fl/fl</sup>* lungs exhibit largely normal lung morphology. **C**, *LSL-Kras/Prkci<sup>fl/fl</sup>* mice exhibit reduced lung hyperplasias. **Columns**, mean; **bars**, SE ( $n = 6$ ); \*,  $P < 0.05$ . **D**, *LSL-Kras/Prkci<sup>fl/fl</sup>* mice exhibit reduced lung tumor formation. **Columns**, mean; **bars**, SE ( $n = 12$ ); \*,  $P = 0.007$ .

## Materials and Methods

**Generation and AdCre treatment of *LSL-Kras/Prkci<sup>fl/fl</sup>* mice.** *LSL-Kras* mice (B6.129), generated as previously described (5), were mated to mice harboring a floxed *Prkci* allele (*Prkci<sup>fl</sup>* mice) to generate bitransgenic *LSL-Kras/Prkci<sup>fl/fl</sup>* mice. Nontransgenic littermates served as controls in all experiments. Mice (6–8 wk of age) were administered AdCre ( $1.5 \times 10^8$  IFU/mL) by intratracheal instillation in two 50- $\mu$ L aliquots as described previously (15). All animal experiments were approved by the Institutional Animal Care and Use Committee of Mayo Clinic.

**Histology and immunohistochemistry.** Mice were sacrificed, exsanguinated, and the lungs perfused with 10% buffered formalin through the right ventricle. The trachea was intubated and instilled with an additional 3 mL of 10% buffered formalin. The lungs were removed intact and fixed overnight in 10% buffered formalin. For histologic analysis, lungs were embedded in paraffin, serially sectioned (5  $\mu$ m) and stained with H&E.

Immunohistochemical analysis was performed as described (10). Mouse PKC $\iota$  was detected using a PKC $\iota$  antibody (Santa Cruz Biotechnology) and visualized using the Envision Plus Dual Labeled Polymer Kit following the instructions of the manufacturer (DAKO). In some experiments, the antibody was incubated overnight at 4°C with a 200-fold molar excess of PKC $\iota$  peptide (Santa Cruz Biotechnology) prior to use in immunohistochemistry to confirm antibody specificity. Slide images were captured and analyzed using the ScanScope scanner and ImageScope software (Aperio Technologies).

**BASC isolation and culture.** Lung epithelial cells were isolated as described (16). Red blood cells (RBC) were lysed in RBC lysis buffer (StemCell Technologies) and BASCs isolated using the EasySep immunomagnetic cell selection procedure (Stem Cell Technologies). Briefly, CD45<sup>pos</sup> Pecam<sup>pos</sup> cells were selected out using primary biotinylated antibodies anti-CD45 (BD PharMingen) and anti-Pecam (BD PharMingen). CD45<sup>neg</sup> Pecam<sup>neg</sup> cells were incubated for 15 min at room temperature



with FITC-conjugated anti-CD34 (BD PharMingen) and Sca1-PE labeling reagent (Stem Cell Technologies). Sca1<sup>pos</sup> CD34<sup>pos</sup> CD45<sup>neg</sup> Pecam<sup>neg</sup> BASCs were selected using the EasySep FITC and PE selection kits. BASCs were resuspended in BEGM (Lonza, without hydrocortisone) containing 10 ng/mL of keratinocyte growth factor (PeproTech) and 5% charcoal-stripped fetal bovine serum and plated at equal densities on Matrigel-coated (BD Biosciences) tissue culture wells. Cultures were infected with AdCre ( $7.5 \times 10^7$  IFU/mL) the day after plating and medium was changed every 2 d thereafter. Bright-field images of BASC colonies were captured on an Olympus IX71 inverted microscope and colony size was determined using Image-Pro Plus 6.3 software (Media Cybernetics).

Immunofluorescence of BASCs in Matrigel culture was performed as described (17) using the following antibodies: rabbit anti-CCSP (Upstate), goat anti-SP-C (Santa Cruz Biotechnology), rabbit anti-Ki67 (Abcam), Alexa Fluor 488 donkey anti-rabbit IgG, Alexa Fluor 568 donkey anti-goat IgG, and Alexa Fluor 594 goat anti-rabbit IgG (Molecular Probes). Samples were mounted using ProLong Gold anti-fade reagent with 4',6-diamidino-2-phenylindole (Molecular Probes) and observed on a Zeiss 510 LSM confocal laser microscope. Images were analyzed with Adobe Photoshop software (Adobe Systems).

BASC colonies were released from Matrigel culture using BD cell recovery solution (BD Biosciences) and total RNA subjected to quantitative PCR as described (18). RNA quantity and integrity were measured using a NanoDrop ND-1000 spectrophotometer.

**Kras and Prkci allele status.** *Kras* allele status in AdCre-treated BASC cultures and adenomas microdissected from *LSL-Kras/Prkci<sup>fl/fl</sup>* mice was determined by PCR as described (5, 19). *Prkci<sup>fl</sup>* allele status was determined using the following PCR primers: F1, 5'-CACCAACGGGTTTGTCTCT-3'; R1, 5'-CCAGCAAGACAAAACACCAA-3'; R2, 5'-ATTACAGCAGGGCAAACCTGC-3'.

**Treatment of *Kras<sup>LA2</sup>* mice with aurothiomalate.** Three-week-old *Kras<sup>LA2</sup>* mice were given daily i.p. injections of aurothiomalate (Myochrysin, Taylor Pharmaceuticals) at 60 mg/kg/d or vehicle control (0.9%

sodium chloride solution; Sigma-Aldrich) for the indicated time periods. Tumors were analyzed as described above.

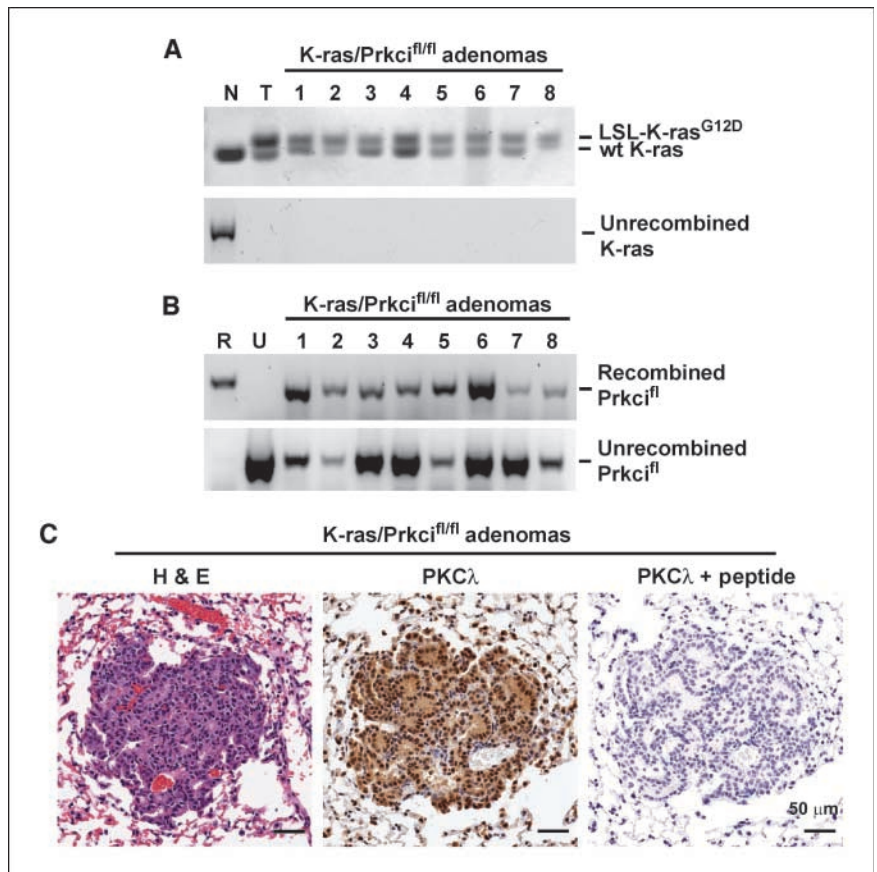
**Detection and analysis of BASCs in mouse lung tissues.** BASCs were detected in formalin-fixed paraffin-embedded mouse lung tissues as described previously (20). Lung tissue sections were stained using goat anti-SPC (Santa Cruz Biotechnology) and rabbit anti-CCSP (Upstate) antibodies diluted in 1% bovine serum albumin (Sigma-Aldrich) at 4°C overnight. The slides were washed thoroughly with PBS and then incubated with Alexa Fluor 488 donkey anti-rabbit IgG and Alexa Fluor 568 donkey anti-goat IgG secondary antibodies (Molecular Probes) diluted in 1% bovine serum albumin for 1 h at room temperature. After washing with PBS, the samples were mounted using ProLong Gold antifade reagent with 4',6-diamidino-2-phenylindole. Immunofluorescence images were captured on an Olympus BX51 fluorescent microscope using DPController and DPManager software (Olympus), and processed in Adobe Photoshop.

**Statistical analysis.** The Cochran-Armitage test was used to compare BASC number and distribution *in vivo* using StatsDirect 2.6.1. The Student's *t* test and one-way ANOVA statistical analyses were performed using SigmaStat 3.5. *P* < 0.05 was considered statistically significant.

## Results

***Prkci* is required for *Kras*-mediated lung tumorigenesis.** To determine whether PKC $\iota$  is involved in lung tumor formation, we used the *LSL-Kras* mouse model in which lung tumors are initiated by AdCre-mediated activation of a conditional oncogenic *Kras* allele (5). Because PKC $\iota$  is overexpressed in primary human NSCLC tumors (10), we assessed whether mouse PKC $\iota$  protein is also highly expressed in lung tumors from *LSL-Kras* mice. Immunohistochemical analysis revealed light staining for mouse PKC $\iota$  in normal lung epithelial cells with more intense staining in lung

**Figure 2.** Lung tumors in *LSL-Kras/Prkci<sup>fl/fl</sup>* mice arise due to incomplete recombination of the *Prkci<sup>fl</sup>* alleles. Genomic DNA from microdissected *LSL-Kras/Prkci<sup>fl/fl</sup>* tumors was analyzed for *Kras* (A) and *Prkci* (B) allele status. Each tumor expresses the recombined (A, top) but not the unrecombined *Kras* allele (A, bottom). Normal lung epithelium (N) and tumor (T) DNA from a *Kras* mouse serve as controls for *Kras* allele recombination. All *LSL-Kras/Prkci<sup>fl/fl</sup>* tumors analyzed contained a recombined *Prkci* allele (B, top) as well as an unrecombined *Prkci* allele (B, bottom), indicating incomplete deletion of the conditional *Prkci<sup>fl</sup>* alleles. Recombined (R) and unrecombined (U) *Prkci* allele controls. C, *LSL-Kras/Prkci<sup>fl/fl</sup>* tumors express mouse PKC $\iota$  protein. Adjacent sections were stained with H&E (left), PKC $\iota$  antibody (middle), or with PKC $\iota$  antibody in the presence of PKC $\iota$  peptide to verify the specificity of staining (right).



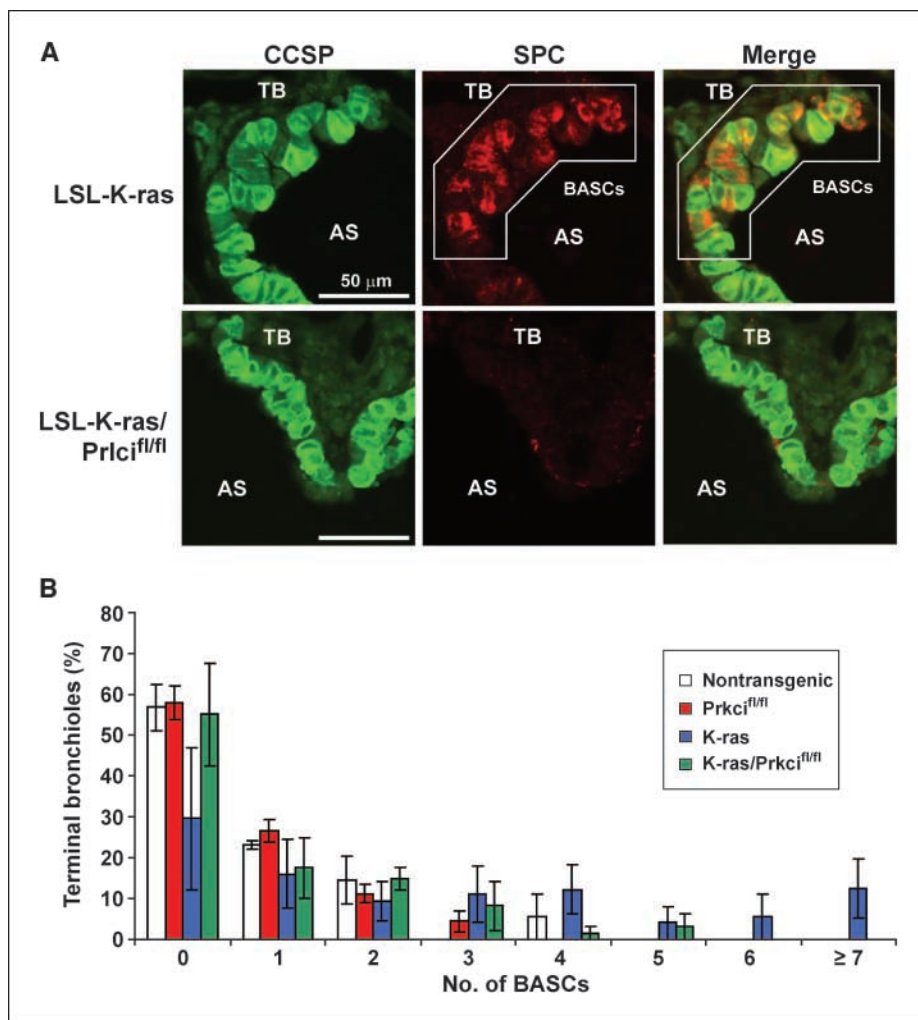


**Figure 3.** *Prkci* is necessary for *Kras*-mediated expansion of BASCs *in vivo*. *LSL-Kras* and *LSL-Kras/Prkci<sup>fl/fl</sup>* mice were harvested 12 wk after intratracheal instillation of AdCre. Lung tissue sections were subjected to immunofluorescence as described in the Materials and Methods. **A**, expansion of CCSP (green) and SPC (red) double-positive BASCs (outlined) is evident within the TBs of *LSL-Kras* mice (top). Clara cells within the bronchioles stain positive for CCSP but negative for SPC. AS, alveolar space. BASC expansion was not observed in *LSL-Kras/Prkci<sup>fl/fl</sup>* mice (bottom). **B**, quantitative analysis of TBs for BASCs in lungs from nontransgenic, *Prkci<sup>fl/fl</sup>*, *LSL-Kras*, and *LSL-Kras/Prkci<sup>fl/fl</sup>* mice. Columns, percentage of TBs; bars, SE. Statistical analysis revealed a significant increase in BASC number and BASC/TB in *LSL-Kras* mice compared with nontransgenic, *Prkci<sup>fl/fl</sup>*, or *LSL-Kras/Prkci<sup>fl/fl</sup>* mice ( $P < 0.0001$ ). No statistically significant difference in BASC number or distribution was observed between nontransgenic, *Prkci<sup>fl/fl</sup>*, and *LSL-Kras/Prkci<sup>fl/fl</sup>* mice.

tumor cells from *LSL-Kras* mice (Fig. 1A, right). Thus, mouse PKC $\iota$  is highly expressed in *Kras*-initiated lung tumors in mice.

We have shown that PKC $\iota$  is required for transformed growth and invasion of human NSCLC cells *in vitro* and tumorigenicity *in vivo* (9, 10). To assess the role of PKC $\iota$  in oncogenic *Kras*-initiated lung tumorigenesis, we crossed mice harboring a conditional knockout *Prkci* allele (*Prkci<sup>fl/fl</sup>*) with *LSL-Kras* mice to generate bitransgenic *LSL-Kras/Prkci<sup>fl/fl</sup>* mice. In *LSL-Kras/Prkci<sup>fl/fl</sup>* mice, intratracheal instillation of AdCre leads to simultaneous Cre-mediated activation of the oncogenic *Kras* allele and inactivation of the *Prkci<sup>fl/fl</sup>* alleles in the same target cells within the lung. Twelve weeks following AdCre administration, *LSL-Kras* and *LSL-Kras/Prkci<sup>fl/fl</sup>* mice were assessed for lung hyperplasias and lung tumors (Fig. 1B). As expected, *LSL-Kras* mice developed numerous tumors visible on the surface of the lung (Fig. 1B, top left, arrows). In contrast, *LSL-Kras/Prkci<sup>fl/fl</sup>* mice exhibited few visible tumors (Fig. 1B, bottom left). Pathologic examination revealed that *LSL-Kras* mice develop multiple focal adenomas often surrounding bronchioles (Fig. 1B, top middle and right, arrows), whereas *LSL-Kras/Prkci<sup>fl/fl</sup>* mice exhibit largely normal lung morphology and fewer lesions (Fig. 1B, bottom middle and right). Analysis also revealed a significant reduction in both hyperplasias (Fig. 1C) and adenomas (Fig. 1D) in *LSL-Kras/Prkci<sup>fl/fl</sup>* mice when compared with *LSL-Kras* mice. Thus, genetic deletion of *Prkci*

inhibits hyperplasia and subsequent tumor formation, indicating a role for *Prkci* in an early step of *Kras*-mediated lung tumorigenesis.

Because *LSL-Kras/Prkci<sup>fl/fl</sup>* mice formed some lung tumors, albeit in significantly reduced numbers, we determined the status of the *Kras* and *Prkci* alleles in tumors formed in these mice. Genomic DNA from tumors microdissected from *LSL-Kras/Prkci<sup>fl/fl</sup>* mice was analyzed for *Kras* and *Prkci* allele status by PCR (Fig. 2A and B). As expected, the *LSL-Kras* allele had undergone Cre-mediated recombination (Fig. 2A, top) with concomitant loss of the unrecombined *Kras* allele (Fig. 2A, bottom) in all of the tumors analyzed. In contrast, each tumor contained a recombined (deleted) *Prkci* allele (Fig. 2B, top), and an unrecombined *Prkci* allele (Fig. 2B, bottom), indicating incomplete deletion of the conditional *Prkci<sup>fl/fl</sup>* alleles. The presence of unrecombined *Prkci* was not due to a contamination of the tumor samples by normal lung as indicated by the absence of the unrecombined *LSL-Kras* allele in the same tumor samples (Fig. 2A, bottom). Furthermore, immunohistochemistry confirmed the expression of mouse PKC $\iota$  protein in these tumors (Fig. 2C). Our data indicate that lung tumors in *LSL-Kras/Prkci<sup>fl/fl</sup>* mice arise due to incomplete recombination of the conditional *Prkci<sup>fl/fl</sup>* alleles. Thus, *Prkci* is critical for *Kras*-induced lung tumorigenesis, and only *Kras*-transformed cells that escape complete inactivation of both *Prkci<sup>fl/fl</sup>* alleles are able to progress in tumorigenesis.

**Prkci is required for *Kras*-mediated expansion of the BASC niche *in vivo*.** Our data indicate that *Prkci* is required for a very early event(s) in *Kras*-mediated oncogenesis *in vivo*. *Kras*-mediated lung tumorigenesis in the *LSL-Kras* mouse model is thought to be initiated by clonal expansion of BASCs, the putative cell of origin of *Kras*-initiated lung tumorigenesis (8). Therefore, we next assessed whether *Prkci* deficiency affects the expansion of BASCs induced by *Kras in vivo*. BASCs are identified in tissue sections at the BADJ by dual immunofluorescence for SPC and CCSP (Fig. 3A). AdCre-treated *LSL-Kras* mice exhibit frequent clusters of SPC/CCSP–double-positive BASCs at BADJs indicative of BASC expansion (Fig. 3A, top). In contrast, *LSL-Kras/Prkci<sup>fl/fl</sup>* mice exhibit significantly fewer BASCs at the BADJs (Fig. 3A, bottom). Quantitative analysis of sections from AdCre-treated nontransgenic, *LSL-Kras* and *LSL-Kras/Prkci<sup>fl/fl</sup>* mice revealed a significant increase in the percentage of TBs containing one or more BASCs, and in the average number of

BASCs/TB in *LSL-Kras* mice when compared with nontransgenic mice (Fig. 3B). *LSL-Kras/Prkci<sup>fl/fl</sup>* mice exhibited a significant inhibition in *Kras*-mediated BASC expansion, such that the number and distribution of BASCs in these mice was indistinguishable from that of nontransgenic mice (Fig. 3B). Furthermore, AdCre-treated *Prkci<sup>fl/fl</sup>* mice exhibited no difference in BASC number or distribution compared with nontransgenic mice, indicating that *Prkci* deficiency does not overtly affect the BASC niche in the absence of oncogenic *Kras* (Fig. 3B). Thus, *Prkci* is necessary for *Kras*-mediated BASC expansion *in vivo*, linking the effect of *Prkci*-deficiency on BASC expansion with lung tumorigenesis. Furthermore, the inhibitory effect of *Prkci* deficiency on lung tumorigenesis is not due to a decrease in the number of BASCs in *LSL-Kras/Prkci<sup>fl/fl</sup>* mice.

**Oncogenic *Kras* induces the expression of PKC $\zeta$  and *Prkci*-dependent proliferative signaling in BASCs *in vitro*.** To further explore the role of *Prkci* in BASC expansion, we isolated

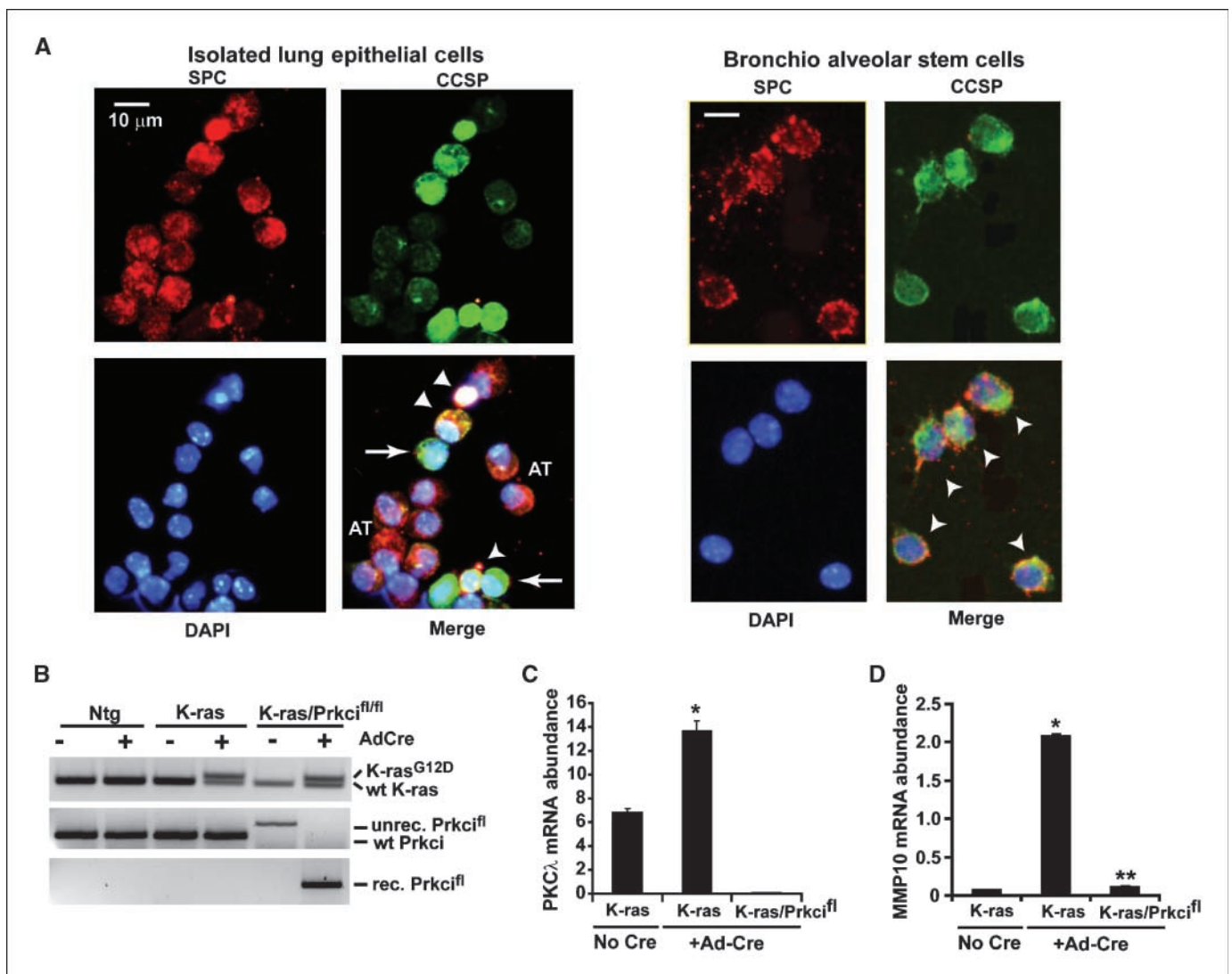


**Figure 4.** *Kras* induces PKC $\zeta$  expression and activates oncogenic *Prkci*-mediated signaling in BASCs *in vitro*. **A**, immunofluorescence staining of isolated lung epithelial cells (left) and purified BASCs (right) from *LSL-Kras* mice for CCSP (green), SPC (red), and 4',6-diamidino-2-phenylindole (DAPI, blue). SPC-positive AT2 cells (AT), CCSP-positive Clara cells (arrows), and SPC/CCSP–double-positive BASCs (arrowheads). **B**, *LSL-Kras* and *Prkci<sup>fl/fl</sup>* allele status in BASCs isolated from nontransgenic, *LSL-Kras*, and *LSL-Kras/Prkci<sup>fl/fl</sup>* mice in the presence and absence of AdCre. The conditional *Kras* and *Prkci* alleles are efficiently recombined in the presence of AdCre. **C**, *Kras* induces PKC $\zeta$  mRNA expression in BASCs but not *LSL-Kras/Prkci<sup>fl/fl</sup>* mice. **D**, *Kras* induces MMP10 mRNA in BASCs but not from *LSL-Kras/Prkci<sup>fl/fl</sup>* mice. Columns, mean of triplicate determinations; bars, SE (C and D). Results are representative of four independent experiments with similar results. \*,  $P < 0.05$ , statistically significant difference from *LSL-Kras* in the absence of Cre; \*\*,  $P < 0.05$ , statistically significant difference from *LSL-Kras*.



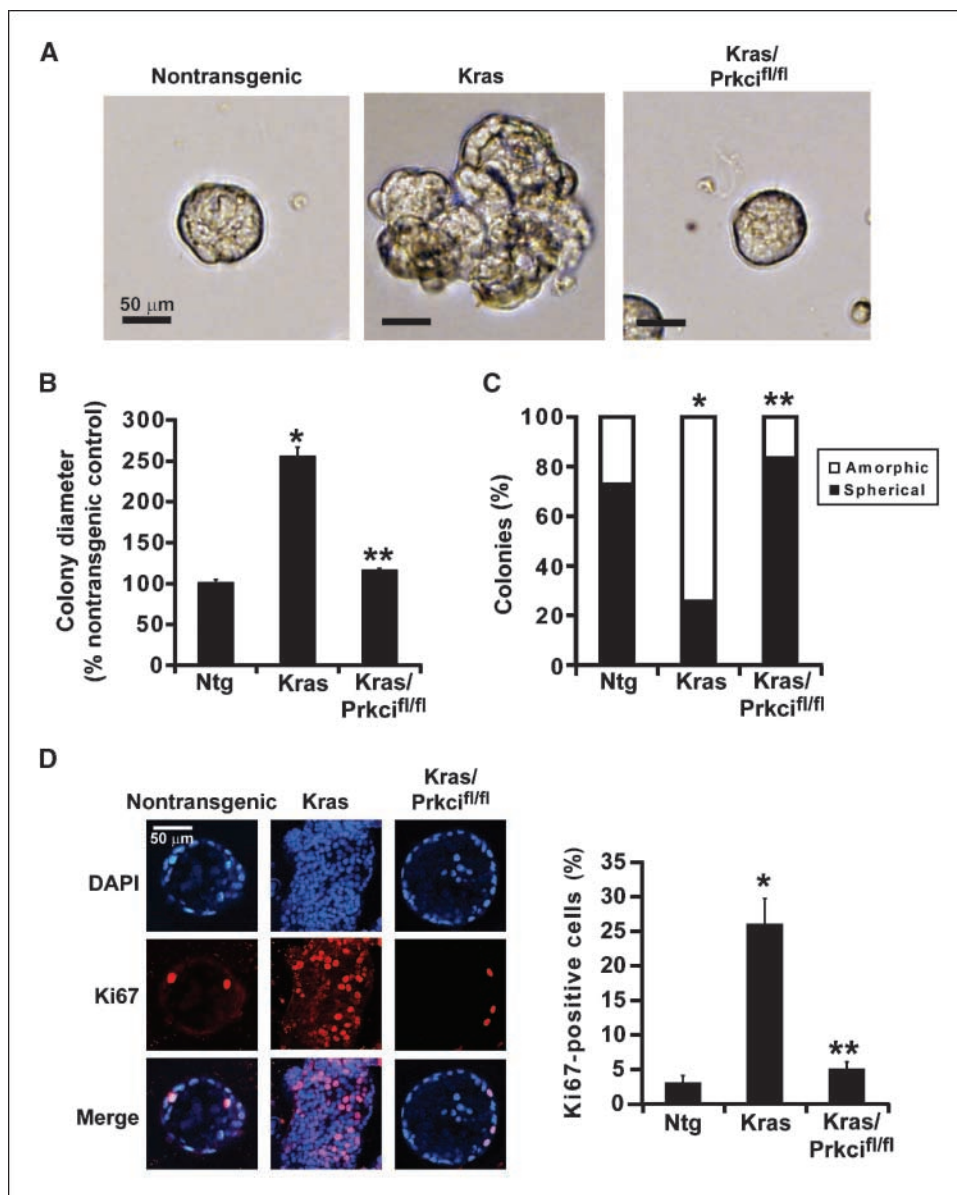


**Figure 5.** *Kras* induces *Prkci*-dependent BASC expansion and morphologic transformation *in vitro*. BASCs from nontransgenic, *LSL-Kras*, and *LSL-Kras/Prkci<sup>fl/fl</sup>* mice were treated with AdCre and plated in three-dimensional Matrigel culture. **A**, photomicrographs of cultures after 4 d. BASC colonies were analyzed for diameter (**B**) and morphology (**C**). **B**, columns, mean percentage of nontransgenic controls; bars, SE. **C**, columns, mean percentage of colonies with spherical (filled columns) or amorphic (open columns) morphology; \*, statistically significant difference from nontransgenic; \*\*,  $P < 0.0001$ , statistically significant difference from *LSL-Kras*. There was no statistically significant difference in colony diameter or morphology between nontransgenic and *LSL-Kras/Prkci<sup>fl/fl</sup>* colonies. **D**, confocal microscopy of BASC colonies stained for 4',6-diamidino-2-phenylindole (DAPI) and Ki67 (left). Quantitative analysis of Ki67 staining (right). Columns, mean percentage of Ki67-positive cells; bars, SE; \*, statistically significant difference from nontransgenic; \*\*,  $P < 0.05$ , statistically significant difference from *LSL-Kras*.

and established BASCs from nontransgenic, *LSL-Kras*, and *LSL-Kras/Prkci<sup>fl/fl</sup>* mice in primary culture using established procedures (8). Isolated lung epithelial cell populations consisted of a mixture of SPC-single positive AT2 cells (Fig. 4A, left, AT), CCSP-single positive Clara cells (Fig. 4A, left, arrows), and SPC/CCSP-double-positive BASCs (Fig. 4A, left, arrowheads). This BASC population was enriched based on positive staining for the stem cell markers Sca1 and CD34. Consistent with previous reports, >95% of the cells remaining after this selection stained double-positive for the BASC markers SPC and CCSP (Fig. 4A, right). Purified BASCs from nontransgenic, *LSL-Kras* and *LSL-Kras/Prkci<sup>fl/fl</sup>* mice were treated with AdCre, and efficient recombination of the *LSL-Kras* and *Prkci<sup>fl</sup>* alleles was confirmed by PCR (Fig. 4B). Consistent with our finding that mouse PKC $\iota$  protein expression is elevated in lung tumors from *LSL-Kras* mice, AdCre treatment of BASCs from *LSL-Kras* mice induced a significant increase in PKC $\iota$  mRNA abundance, whereas BASCs from *LSL-Kras/Prkci<sup>fl/fl</sup>* mice, as expected, expressed no detectable PKC $\iota$  mRNA (Fig. 4C). We previously identified matrix metalloproteinase 10 (MMP10) as a

transcriptional target of the oncogenic PKC $\iota$ -Par6-Rac1 signaling axis (11), and MMP10 has also been identified as a transcriptional target of oncogenic *Kras* (21, 22). Therefore, we assessed MMP10 expression in BASCs from *LSL-Kras* and *LSL-Kras/Prkci<sup>fl/fl</sup>* mice by quantitative PCR. MMP10 mRNA was induced in BASCs from *LSL-Kras* mice but not from *LSL-Kras/Prkci<sup>fl/fl</sup>* mice after AdCre treatment (Fig. 4D). Thus, oncogenic *Kras* activates oncogenic PKC $\iota$  signaling in BASCs, and this signaling is inhibited in BASCs from *LSL-Kras/Prkci<sup>fl/fl</sup>* mice.

**Oncogenic *Kras*-mediated BASC expansion and morphologic transformation requires *Prkci*.** Because BASCs expand and initiate *Kras*-mediated tumors *in vivo* (8, 23), we assessed BASCs from *LSL-Kras* and *LSL-Kras/Prkci<sup>fl/fl</sup>* mice for proliferative expansion and morphologic transformation after the induction of oncogenic *Kras in vitro* (Fig. 5). BASCs from nontransgenic mice treated with AdCre form colonies of organized spherical structures when plated in three-dimensional Matrigel culture (Fig. 5A, left). In contrast, BASCs from *LSL-Kras* mice grow as large amorphic, disorganized colonies (Fig. 5A, middle). Interestingly, BASCs from

*LSL-Kras/Prkci<sup>fl/fl</sup>* mice form spherical colonies similar in size and morphology to those from nontransgenic mice (Fig. 5A, right). Quantitative analysis revealed that BASCs from *LSL-Kras* mice form structures of larger average diameter (Fig. 5B) and more amorphous shape (Fig. 5C) than BASCs from either nontransgenic or *LSL-Kras/Prkci<sup>fl/fl</sup>* mice. Thus, the change in colony size and morphology observed in *LSL-Kras* BASCs requires both *Kras* and *Prkci*. Immunofluorescent confocal microscopy revealed that BASCs from nontransgenic and *LSL-Kras/Prkci<sup>fl/fl</sup>* mice form hollow spheres consisting of a single layer of epithelial cells with a low proliferative index; in contrast, BASCs from *LSL-Kras* mice form solid masses of highly proliferative cells (Fig. 5D, left). Quantitative analysis showed a significant increase in proliferation of *LSL-Kras* BASCs (percentage of cells staining positive for Ki67) when compared with nontransgenic BASCs and that this increase was not seen in *LSL-Kras/Prkci<sup>fl/fl</sup>* BASCs (Fig. 5D, right). Thus, oncogenic *Kras* induces *Prkci*-dependent proliferative expansion and morphologic changes associated with cellular transformation of BASCs *in vitro*.

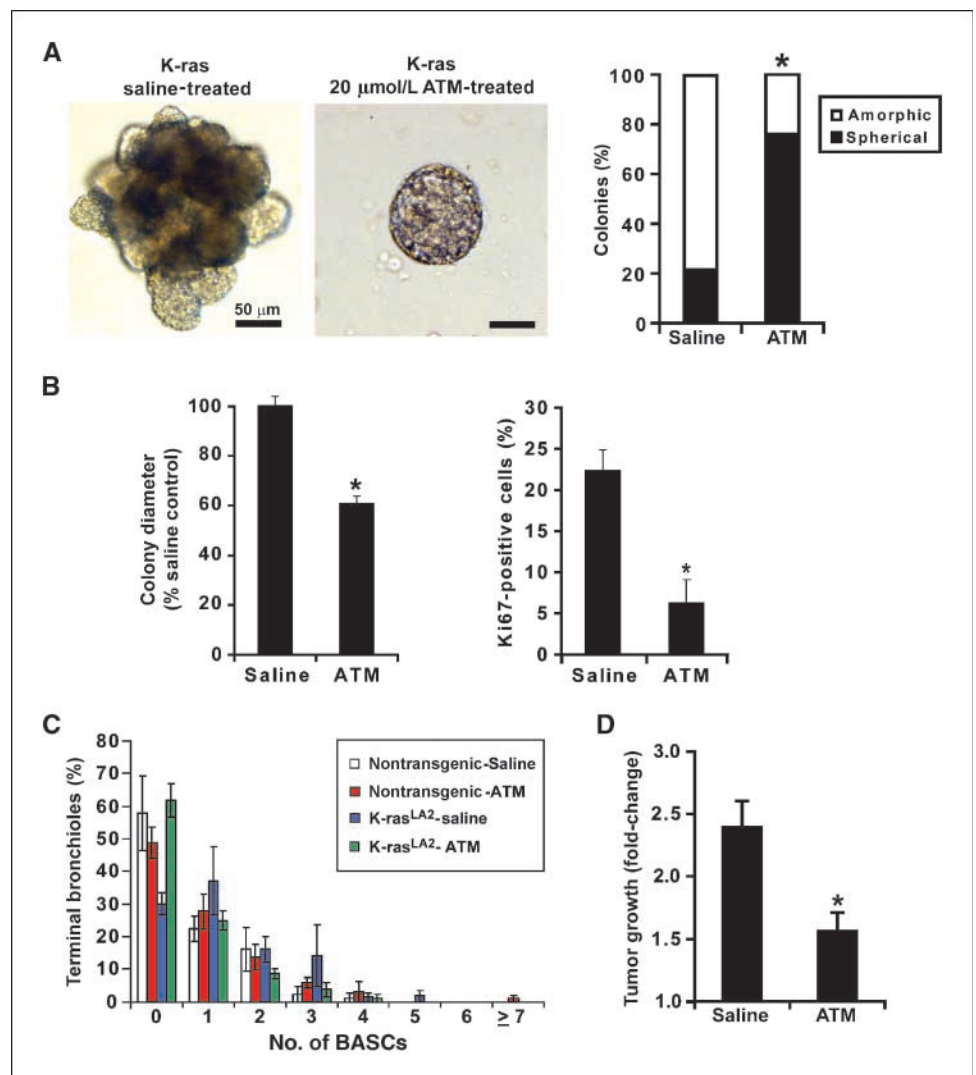
BASCs exhibit self-renewal and the ability to differentiate into bronchiolar Clara cells and AT2 cells (8). Therefore, we assessed whether the increase in proliferation observed in *LSL-Kras* BASC cultures *in vitro* was due to the expansion of undifferentiated BASCs, or alternatively, the induction of lineage-specific differen-

tiation of BASC into single positive Clara and/or AT2 cells. Confocal immunofluorescence microscopy revealed that BASC colonies from nontransgenic, *LSL-Kras*, and *LSL-Kras/Prkci<sup>fl/fl</sup>* mice are made up predominantly of SPC/CCSP-double-positive staining BASCs (Supplemental Fig. S1), indicating that *Kras* induces *Prkci*-dependent BASC expansion.

#### Aurothiomalate blocks *Kras*-mediated, *Prkci*-dependent BASC expansion and morphologic transformation *in vitro*.

We recently identified aurothiomalate as a highly selective small molecule inhibitor of oncogenic PKC $\lambda$  signaling that exhibits potent antitumor activity against human NSCLC cells (12, 13). Because *Prkci* is necessary for *Kras*-mediated BASC expansion and morphologic transformation *in vivo* and *in vitro*, we assessed whether aurothiomalate inhibits the effects of *Kras* on BASCs. BASCs from *LSL-Kras* mice were transduced with AdCre and plated in three-dimensional Matrigel culture in the presence of 20  $\mu$ mol/L of aurothiomalate or diluent (saline; Fig. 6A, left and middle). As expected, saline-treated BASCs formed large amorphous colonies; in contrast, aurothiomalate-treated cells formed small spherical colonies similar to those formed by BASCs from nontransgenic and *LSL-Kras/Prkci<sup>fl/fl</sup>* mice (Fig. 6A, right). Analysis revealed that saline-treated BASCs form significantly larger colonies than aurothiomalate-treated BASCs (Fig. 6B, left), which is associated

**Figure 6.** Aurothiomalate inhibits *Kras*-mediated BASC expansion and morphologic transformation *in vitro* and tumor growth *in vivo*. **A**, morphology of BASCs from *LSL-Kras* mice in the presence of 20  $\mu$ mol/L of aurothiomalate (middle) or saline (left). Analysis of BASC colony morphology in the presence and absence of aurothiomalate (right). \*,  $P < 0.001$ , statistically significant difference from BASCs cultured in the absence of aurothiomalate. **B**, colony diameter (left) and Ki67 staining (right) of BASCs in the presence and absence of aurothiomalate. Columns, mean; bars, SE; \*,  $P = 0.01$ , statistically significant difference from BASCs in the absence of aurothiomalate. **C**, aurothiomalate blocks *Kras*-mediated BASC expansion *in vivo*. Nontransgenic and *Kras<sup>LA2</sup>* mice were treated with aurothiomalate or saline for 3 wk, and lungs were analyzed for BASC number and distribution as described in Fig. 3. Statistical analysis revealed a significant increase in BASC number and in the mean number of BASC/TB in saline-treated *Kras<sup>LA2</sup>* mice when compared with aurothiomalate-treated *Kras<sup>LA2</sup>* mice, nontransgenic mice treated with aurothiomalate, or nontransgenic mice treated with saline ( $P < 0.0001$ ). No statistically significant differences in BASC number or distribution were observed between saline-treated nontransgenic, aurothiomalate-treated nontransgenic, and aurothiomalate-treated *Kras<sup>LA2</sup>* mice. **D**, aurothiomalate inhibits lung tumor growth in *Kras<sup>LA2</sup>* mice. Columns, mean fold-change in average tumor size after 6 wk in the presence of aurothiomalate or saline; bars, SE; \*,  $P = 0.003$ , statistically significant difference from saline-treated *Kras<sup>LA2</sup>* mice.



with an increased proliferative index compared with aurothiomalate-treated BASCs (Fig. 6B, right). Thus, aurothiomalate, like genetic loss of *Prkci*, blocks *Kras*-mediated proliferative expansion and morphologic transformation of BASCs.

**Aurothiomalate inhibits *Kras*-mediated BASC expansion and lung tumorigenesis *in vivo*.** We next assessed the effect of aurothiomalate on BASC expansion and tumor formation in *Kras<sup>LA2</sup>* mice harboring a latent oncogenic *Kras* allele activated by spontaneous recombination *in vivo* (7). Nontransgenic and *Kras<sup>LA2</sup>* mice were treated with either aurothiomalate (60 mg/kg/d) or diluent (saline) for 3 weeks, at which time, mice were sacrificed and assessed for BASC number and distribution as described above. Aurothiomalate has no demonstrable effect on BASC number or distribution in nontransgenic mice (Fig. 6C), consistent with our finding that *Prkci*-deficiency does not overtly affect BASCs in the absence of oncogenic *Kras in vivo*. In contrast, saline-treated *Kras<sup>LA2</sup>* mice exhibit a significant increase in BASCs/TB that is inhibited by aurothiomalate (Fig. 6C). Consistent with the inhibitory effect of aurothiomalate on BASC expansion, aurothiomalate-treated *Kras<sup>LA2</sup>* mice exhibited a decrease in tumor growth when compared with saline-treated mice after a 6-week course of aurothiomalate treatment (Fig. 6D). Therefore, similar to genetic loss of *Prkci*, aurothiomalate blocks *Kras*-mediated BASC expansion and inhibits subsequent lung tumor growth *in vivo*.

## Discussion

The PKC $\zeta$  oncogene plays a requisite role in the maintenance of the transformed phenotype of NSCLC cells *in vitro* and *in vivo* (10). However, the present study is the first to assess the role of PKC $\zeta$  in lung tumor formation. Our data firmly establish that genetic disruption of *Prkci* has a profound inhibitory effect on oncogenic *Kras*-mediated lung tumor development. Although *Prkci*-deficient mice still develop lung hyperplasias and lung tumors in response to oncogenic *Kras*, albeit at a dramatically reduced incidence, molecular analysis of these tumors shows that these lesions invariably retain an unrecombined *Prkci* allele and express mouse PKC $\zeta$  protein. These data argue that *Prkci* is absolutely required for a very early step in *Kras*-mediated lung tumorigenesis, such that only the occasional *Kras*-transformed cell that escapes complete recombination of both *Prkci<sup>f</sup>* alleles (and retains PKC $\zeta$  expression) is competent to progress in tumorigenesis.

The inhibitory effect of *Prkci* deletion on tumorigenesis is reflected in a severe defect in the ability of *Prkci*-deficient BASCs to expand and undergo *Kras*-mediated transformation *in vitro*. Thus, *Prkci* is necessary for the first identifiable step in *Kras*-mediated tumorigenesis involving expansion and transformation of the putative lung cancer stem cell in the mouse. Our data provide important new insight into a key pathway involved in BASC

expansion in response to an oncogenic stimulus; i.e., the oncogenic PKC $\zeta$  signaling axis. Our data places *Prkci* among a small cadre of genes known to play a critical role in oncogene-induced BASC expansion, including the polycomb group member Bmi1 (23), p38 MAPK (24), the cyclin-dependent kinase inhibitor p27 (25), and phosphatidylinositol-3-kinase (20).

By virtue of its role in BASC expansion, PKC $\zeta$  is an attractive target for therapeutic intervention in lung cancer. Aurothiomalate, a highly selective inhibitor of oncogenic PKC $\zeta/\lambda$  signaling (12, 13), potently blocks *Kras*-mediated expansion and morphologic transformation of BASCs *in vitro* and *in vivo*, and inhibits lung tumor growth *in vivo*. Our data indicate that aurothiomalate suppresses oncogene-mediated tumor induction, at least in part, through inhibition of the expansion of lung cancer stem cells. These data have important implications for the use of aurothiomalate in cancer treatment. A population of cells within human lung tumors has been identified that exhibits properties of lung cancer stem cells similar to those exhibited by BASCs (26, 27). These lung cancer stem cells are capable of self-renewal, serial passage as tumors in immunocompromised mice, and differentiation into highly proliferative tumor cells (26, 27). Based on these properties, lung cancer stem cells are thought to be responsible for the initiation and long-term maintenance of human lung tumors, much as BASCs are in the mouse lung. Given their central role in tumorigenesis, lung cancer stem cells must be therapeutically targeted to achieve lasting antitumor responses. Unfortunately, lung cancer stem cells exhibit intrinsic resistance to commonly used cytotoxic agents (26, 27). Our present results show that aurothiomalate exhibits potent antiproliferative activity toward the tumor stem cell niche in a relevant preclinical lung cancer model. Future studies will be required to assess whether aurothiomalate has similar antiproliferative effects on human lung cancer stem cells isolated from primary human lung tumors.

## Disclosure of Potential Conflicts of Interest

No potential conflicts of interest were disclosed.

## Acknowledgments

Received 6/5/09; revised 7/10/09; accepted 7/20/09; published OnlineFirst 9/8/09.

**Grant support:** National Cancer Institute CA084136-12, the V-Foundation, and the American Lung Association/LUNGevity (A.P. Fields); and a Ruth A. Kirschstein Postdoctoral Fellowship Award CA115160 from the National Cancer Institute (R.P. Regala).

The costs of publication of this article were defrayed in part by the payment of page charges. This article must therefore be hereby marked *advertisement* in accordance with 18 U.S.C. Section 1734 solely to indicate this fact.

The authors thank Erin Donovan and Suzie Randle for assistance with animal husbandry procedures, and Brandy Edenfield for immunohistochemical analysis of lung tissues.

## References

- Jemal A, Siegel R, Ward E, et al. Cancer statistics, 2008. *CA Cancer J Clin* 2008;58:71-96.
- Schiller JH. Current standards of care in small-cell and non-small-cell lung cancer. *Oncology* 2001;61 Suppl 1:3-13.
- Gazdar AF, Minna JD. Molecular detection of early lung cancer. *J Natl Cancer Inst* 1999;91:299-301.
- Salgia R, Skarin AT. Molecular abnormalities in lung cancer. *J Clin Oncol* 1998;16:1207-17.
- Jackson EL, Willis N, Mercer K, et al. Analysis of lung tumor initiation and progression using conditional expression of oncogenic *Kras*. *Genes Dev* 2001;15:3243-8.
- Meuwissen R, Linn SC, van der Valk M, Mooij WJ, Berns A. Mouse model for lung tumorigenesis through *Cre/lox* controlled sporadic activation of the *Kras* oncogene. *Oncogene* 2001;20:6551-8.
- Johnson L, Mercer K, Greenbaum D, et al. Somatic activation of the *Kras* oncogene causes early onset lung cancer in mice. *Nature* 2001;410:1111-6.
- Kim CF, Jackson EL, Woolfenden AE, et al. Identification of bronchioalveolar stem cells in normal lung and lung cancer. *Cell* 2005;121:823-35.
- Regala RP, Weems C, Jamieson L, Copland JA, Thompson EA, Fields AP. Atypical protein kinase C $\zeta$  plays a critical role in human lung cancer cell growth and tumorigenicity. *J Biol Chem* 2005;280:31109-15.
- Regala RP, Weems C, Jamieson L, et al. Atypical protein kinase C $\zeta$  is an oncogene in human non-small cell lung cancer. *Cancer Res* 2005;65:8905-11.



11. Frederick LA, Matthews JA, Jamieson L, et al. Matrix metalloproteinase-10 is a critical effector of protein kinase C $\alpha$ -mediated lung cancer. *Oncogene* 2008; 27:4841–53.
12. Erdogan E, Lamark T, Stallings-Mann M, et al. Aurothiomalate inhibits transformed growth by targeting the PBI domain of atypical protein kinase C. *J Biol Chem* 2006;281:28450–9.
13. Stallings-Mann M, Jamieson L, Regala RP, Weems C, Murray NR, Fields AP. A novel small-molecule inhibitor of protein kinase C $\zeta$  blocks transformed growth of non-small-cell lung cancer cells. *Cancer Res* 2006;66:1767–74.
14. Banan A, Fields JZ, Farhadi A, Talmage DA, Zhang L, Keshavarzian A. The  $\beta$ 1 isoform of protein kinase C mediates the protective effects of epidermal growth factor on the dynamic assembly of F-actin cytoskeleton and normalization of calcium homeostasis in human colonic cells. *J Pharmacol Exp Ther* 2002;301:852–66.
15. Fasbender ALJ, Walters RW, Moninger TO, Zabner J, Welsh MJ. Incorporation of adenovirus in calcium phosphate precipitates enhances gene transfer to airway epithelia *in vitro* and *in vivo*. *J Clin Invest* 1998;102:184–93.
16. Rice WR, Conkright JJ, Na CL, Ikegami M, Shannon JM, Weaver TE. Maintenance of the mouse type II cell phenotype *in vitro*. *Am J Physiol Lung Cell Mol Physiol* 2002;283:L256–64.
17. Debnath J, Muthuswamy SK, Brugge JS. Morphogenesis and oncogenesis of MCF-10A mammary epithelial acini grown in three-dimensional basement membrane cultures. *Methods* 2003;30:256–68.
18. Regala RP, Thompson EA, Fields AP. Atypical protein kinase C $\zeta$  expression and aurothiomalate sensitivity in human lung cancer cells. *Cancer Res* 2008;68:5888–95.
19. Kissil JL, Walmsley MJ, Hanlon L, et al. Requirement for Rac1 in a Kras induced lung cancer in the mouse. *Cancer Res* 2007;67:8089–94.
20. Yang Y, Iwanaga K, Raso MG, et al. Phosphatidylinositol 3-kinase mediates bronchioalveolar stem cell expansion in mouse models of oncogenic Kras-induced lung cancer. *PLoS One* 2008;3:e2220.
21. Tchernitsa OI, Sers C, Zuber J, et al. Transcriptional basis of KRAS oncogene-mediated cellular transformation in ovarian epithelial cells. *Oncogene* 2004;23:4536–55.
22. Zuber J, Tchernitsa OI, Hinzmann B, et al. A genome-wide survey of RAS transformation targets. *Nat Genet* 2000;24:144–52.
23. Dovey JS, Zacharek SJ, Kim CF, Lees JA. Bmi1 is critical for lung tumorigenesis and bronchioalveolar stem cell expansion. *Proc Natl Acad Sci U S A* 2008;105:11857–62.
24. Ventura JJ, Tenbaum S, Perdiguer E, et al. p38 $\alpha$  MAP kinase is essential in lung stem and progenitor cell proliferation and differentiation. *Nat Genet* 2007; 39:750–8.
25. Besson A, Hwang HC, Cicero S, et al. Discovery of an oncogenic activity in p27Kip1 that causes stem cell expansion and a multiple tumor phenotype. *Genes Dev* 2007;21:1731–46.
26. Eramo A, Lotti F, Sette G, et al. Identification and expansion of the tumorigenic lung cancer stem cell population. *Cell Death Differ* 2008;15:504–14.
27. Chen YC, Hsu HS, Chen YW, et al. Oct-4 expression maintained cancer stem-like properties in lung cancer-derived CD133-positive cells. *PLoS One* 2008;3:e2637.

# Cancer Research

The Journal of Cancer Research (1916–1930) | The American Journal of Cancer (1931–1940)

## Atypical Protein Kinase C $\alpha$ Is Required for Bronchioalveolar Stem Cell Expansion and Lung Tumorigenesis

Roderick P. Regala, Rebecca K. Davis, Alyssa Kunz, et al.

*Cancer Res* 2009;69:7603-7611. Published OnlineFirst September 8, 2009.

<b>Updated version</b>	Access the most recent version of this article at: doi: <a href="https://doi.org/10.1158/0008-5472.CAN-09-2066">10.1158/0008-5472.CAN-09-2066</a>
<b>Supplementary Material</b>	Access the most recent supplemental material at: <a href="http://cancerres.aacrjournals.org/content/suppl/2009/09/08/0008-5472.CAN-09-2066.DC1">http://cancerres.aacrjournals.org/content/suppl/2009/09/08/0008-5472.CAN-09-2066.DC1</a>

<b>Cited articles</b>	This article cites 27 articles, 11 of which you can access for free at: <a href="http://cancerres.aacrjournals.org/content/69/19/7603.full#ref-list-1">http://cancerres.aacrjournals.org/content/69/19/7603.full#ref-list-1</a>
<b>Citing articles</b>	This article has been cited by 12 HighWire-hosted articles. Access the articles at: <a href="http://cancerres.aacrjournals.org/content/69/19/7603.full#related-urls">http://cancerres.aacrjournals.org/content/69/19/7603.full#related-urls</a>

<b>E-mail alerts</b>	<a href="#">Sign up to receive free email-alerts</a> related to this article or journal.
<b>Reprints and Subscriptions</b>	To order reprints of this article or to subscribe to the journal, contact the AACR Publications Department at <a href="mailto:pubs@aacr.org">pubs@aacr.org</a> .
<b>Permissions</b>	To request permission to re-use all or part of this article, use this link <a href="http://cancerres.aacrjournals.org/content/69/19/7603">http://cancerres.aacrjournals.org/content/69/19/7603</a> . Click on "Request Permissions" which will take you to the Copyright Clearance Center's (CCC) Rightslink site.